Dielectric measurements of nanoliter liquids with a photonic crystal resonator at terahertz frequencies

S. M. Hanham, C. Watts, W. J. Otter, S. Lucyszyn, and N. Klein

---

Articles you may be interested in

Optical and magneto-optical properties of one-dimensional magnetized coupled resonator plasma photonic crystals
Phys. Plasmas **19**, 012503 (2012); 10.1063/1.3677263

Realizing the frequency quality factor product limit in silicon via compact phononic crystal resonators
J. Appl. Phys. **108**, 084505 (2010); 10.1063/1.3475987

Digital resonance tuning of high- Q/V m silicon photonic crystal nanocavities by atomic layer deposition
Appl. Phys. Lett. **91**, 161114 (2007); 10.1063/1.2800312
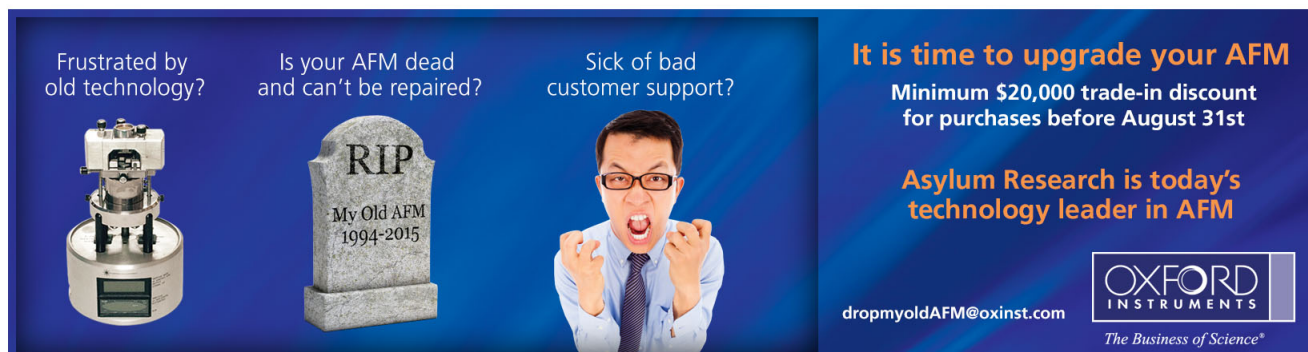
Low-frequency, low-field dielectric spectroscopy of living cell suspensions
J. Appl. Phys. **95**, 3754 (2004); 10.1063/1.1649455

Calculated and measured transmittance of a tunable metallic photonic crystal filter for terahertz frequencies
Appl. Phys. Lett. **83**, 5362 (2003); 10.1063/1.1636822

Dielectric measurements of nanoliter liquids with a photonic crystal resonator at terahertz frequencies

S. M. Hanham,[1,2,a)] C. Watts,[1,2] W. J. Otter,[2,3] S. Lucyszyn,[2,3] and N. Klein[1,2]

[1]Department of Materials, Imperial College London, SW7 2AZ London, United Kingdom
[2]Centre for Terahertz Science and Engineering, Imperial College London, SW7 2AZ London, United Kingdom
[3]Department of Electrical and Electronic Engineering, Imperial College London, SW7 2AZ London, United Kingdom

We present a highly sensitive technique for determining the complex permittivity of nanoliter liquid samples in the terahertz band based on a photonic crystal resonator and microcapillary. Liquids are characterized by using a capillary tube to introduce a $\sim$4 nl liquid sample into the electromagnetic field of a resonant mode confined by an L3 resonant cavity in a high-resistivity silicon photonic crystal slab. Monitoring the perturbation of the resonant frequency and unloaded Q-factor of the resonant mode at 100 GHz and $\sim$5800, respectively, allows a sample's permittivity to be calculated. An analytical model describing the system response based on perturbation theory and quasi-static analysis of the electric field within the capillary is also presented and found to agree well with FEM simulations and experimental measurements of ethanol-water mixtures of various concentrations for low to moderate loss tangents of the liquid samples. We demonstrate the utility of this approach by measuring the complex permittivity of several bioliquids, including suspensions of red and white blood cells. These results represent a step towards a lab-on-a-chip device for the analysis of extremely small quantities of biological, toxic, explosive, and other liquid types at terahertz frequencies. © 2015 Author(s). All article content, except where otherwise noted, is licensed under a Creative Commons Attribution 3.0 Unported License.
[http://dx.doi.org/10.1063/1.4927242]

Measuring the dielectric response of liquids in the terahertz (THz) band is important for a broad range of applications in medicine, biology, and chemistry. The broadband characterization of liquids is typically performed using quasi-optical techniques, where the minimum liquid sample volume is limited by the system's beam spot size and the diffraction limit. Another disadvantage of this approach is that the sensitivity is typically not as good as a resonant technique, where the strength of the light-matter interaction between the resonant mode and liquid analyte can be enhanced in proportion to the resonator's Q-factor.

In the optical region of the electromagnetic (EM) spectrum, photonic crystal (PC) and whispering gallery (WG) mode resonators have been shown to have extremely high sensitivity for biosensing,[1–3] achieving even single molecule sensitivity.[4] In this work, we demonstrate the application of a high Q-factor photonic crystal resonator (PCR) combined with microfluidics for the measurement of the complex permittivity of nanoliter quantities of liquids in the THz band. The use of a PCR allows for a much greater Q-factor ($\sim$5800) and, hence, sensitivity when compared to conventional metal-based cavity resonators, which suffer from substantial ohmic loss at these frequencies. In contrast to sapphire WG mode resonators, the Q-factor is lower,[5,6] but the smaller mode volume of the PCR results in a similar (or even higher) sensitivity.

The design and fabrication of the PCR we employ have been described elsewhere,[7] and here we briefly summarize it. The slab-type PC was fabricated by deep reactive ion etching

a 525 μm thick high resistivity silicon (HRS) substrate to create a hexagonal lattice of holes. The lattice constant (780 μm) and hole radius (235 μm) were chosen to produce a bandgap for TE-like modes centered at 112 GHz with a 26% fractional bandwidth. A resonant cavity is created in the middle of the PC by introducing a defect in the spatial periodicity through the omission of three consecutive holes and the neighboring hole positions were optimized to maximize the Q-factor through minimization of the out-of-plane losses (see Ref. 8 for details). Two W1 waveguide defects in the lattice serve to couple energy between the vector network analyzer's (VNA's) WR10 waveguides and the resonant cavity.

A quartz capillary tube is used to introduce the liquid analyte into the EM field of the PCR resonant mode and is threaded through one of the PC holes closest to the resonant cavity, as shown in Fig. 1(a). The 200 μm outer diameter of the capillary tube is significantly smaller than a wavelength and its presence does not significantly increase scattering loss,[9] with the resonance frequency and unloaded Q-factor being only slightly reduced to 100 GHz and $\sim$5850, respectively. When a liquid is pumped through the capillary tube, there are changes in both the resonant frequency Δf and reciprocal unloaded Q-factor $\Delta(1/Q)$, with respect to air, which directly corresponds to the relative complex permittivity $\epsilon_s = (\epsilon' - i\epsilon'')$ of the liquid analyte. The unloaded Q-factor is calculated from the VNA measured voltage-wave transmission coefficient S_{21} using an algorithm that estimates the Q-factor based on fitting a Q-factor circle in the polar S_{21} plane (see Ref. 10 for details).

A syringe pump was used to flow a range of common solvents: water, methanol, ethanol, and 2-propanol, and

a)Author to whom correspondence should be addressed. Electronic mail: s.hanham@imperial.ac.uk
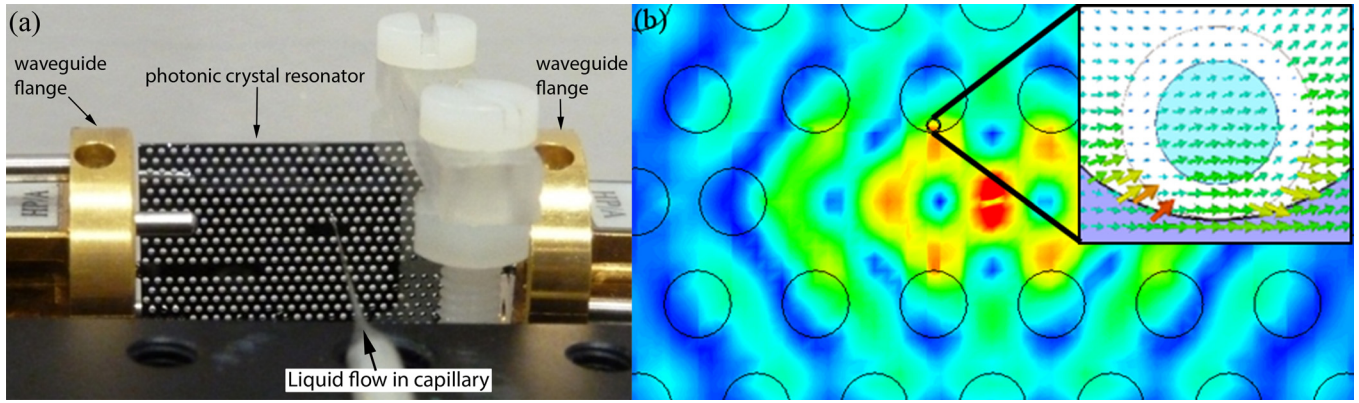
© Author(s) 2015

FIG. 1. (a) A THz PCR supported between two WR10 waveguide flanges of the VNA's frequency multiplier test heads. (b) The simulated electric field distribution of the PCR resonant mode. Inset: close-up view of the field inside the capillary tube when water is present.

ethanol-water solutions of various molar fractions through the capillary tube with a flow rate of $10\,\mu l/min$. Figure 2 shows the resulting change in the resonance frequency and reciprocal Q-factor of the PCR for each of the liquids with respect to a reference measurement of air which had a resonant frequency of 99.054 GHz and Q-factor of 5850. Human blood plasma and two liquid suspensions of red blood cells (RBCs) and white blood cells (WBCs) were also measured and these results will be discussed later.

To enable quantitative permittivity measurements with the PCR, it is necessary to establish a relationship between the perturbation of the resonance parameters $(\Delta f, \Delta(1/Q))$ due to the liquid's interaction with the EM field and the liquid's complex permittivity. Solving this inverse eigenvalue problem of Maxwell's equations is, in general, non-trivial and we describe two approaches for achieving this. The first is to use full-wave electromagnetic simulations to completely characterize the resonant frequency and Q-factor dependency on a sample liquid's permittivity. These simulations are computationally time-intensive and also have the limitation of not easily being able to include the effects of fabrication imperfections, which can affect the sensor's response. To overcome this, we pursue a second approach that involves the fitting of a model derived from perturbation theory to the measured results of liquids with known permittivities.

Perturbation theory can be used to relate the change in the properties of a resonant eigenmode with frequency f_0 to a change in its electric field before (E_0) and after (E_s) the introduction of a sample. Assuming the introduction of the sample results in a change in the permittivity $\Delta\epsilon$ of a small volume of the cavity V_s then the complex form of perturbation theory for a homogeneous, non-magnetic sample is given by[11]

$$\frac{\Delta f}{f_0} + \frac{i}{2}\Delta\left(\frac{1}{Q}\right) \approx -\frac{1}{4W}\iiint_{V_s}\Delta\epsilon E_s . E_0^* dV, \qquad (1)$$

where W represents the total stored energy in the unperturbed resonant eigenmode.

The application of perturbation theory, in general, requires knowledge of the perturbed and unperturbed electric field distribution inside the sample. Since the diameter of the capillary $2a$ is much smaller than the resonant wavelength (i.e., $Re\{\tilde{k}\}2a \ll 1$, where $\tilde{k}$ is the complex wavenumber of the wave inside the liquid), we utilize the quasi-static (QS) approximation and regard the electric field inside the sample as that obtained in the static case. The static field can be determined by solving Laplace's equation for the case of an infinitely long dielectric cylinder of radius a and with a relative complex permittivity ϵ_s representing the liquid, surrounded by the capillary tube represented by relative permittivity ϵ_q. Assuming that the cylinder is located in a uniform background electric field with amplitude E_B and at the center of a cylindrical co-ordinate system (ρ, ϕ), with the cylindrical axis aligned to the z-axis, we derive the following expressions for the electric field distribution:

$$E = E_B\begin{cases} \dfrac{2\epsilon_q}{\epsilon_s + \epsilon_q}\left(\hat{\rho}\,\cos\phi - \hat{\phi}\sin\phi\right), & \rho \le a, \\[2ex] \hat{\rho}\cos\phi\left[1 + \left(\dfrac{a}{\rho}\right)^2\dfrac{\epsilon_s - \epsilon_q}{\epsilon_s + \epsilon_q}\right] - \hat{\phi}\sin\phi\left[1 - \left(\dfrac{a}{\rho}\right)^2\dfrac{\epsilon_s - \epsilon_q}{\epsilon_s + \epsilon_q}\right], & \rho > a. \end{cases} \qquad (2)$$

The inset of Fig. 1(b) shows the electric field in the vicinity of the capillary tube, solved using full-wave electromagnetic simulations.[12]

Now, we use (2) for the electric field distributions inside the capillary tube before (E_0) and after (E_s) introduction of

the liquid into the capillary. Substituting (2) into (1) and carrying out the integration, we obtain

$$\frac{\Delta f}{f_0} + \frac{i}{2}\Delta\left(\frac{1}{Q}\right) \approx -A\frac{\epsilon_s - B}{\epsilon_s + \epsilon_q}, \qquad (3)$$
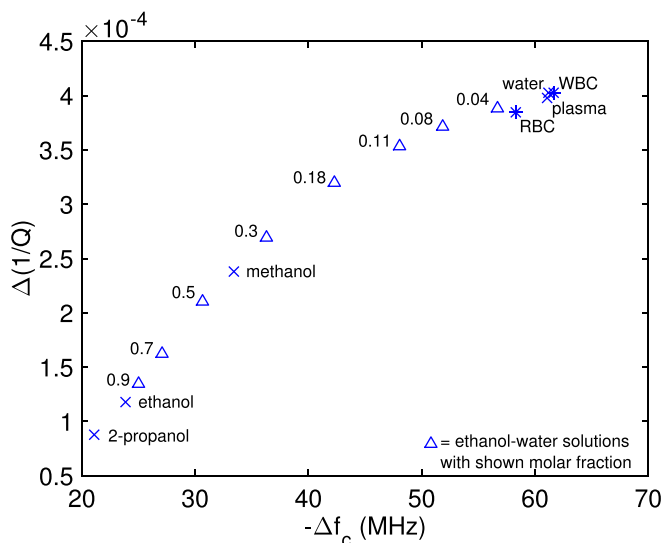
FIG. 2. Perturbation of the PCR's resonance parameters for the liquids: common solvents ($\times$), ethanol-water solutions of varying concentration ($\triangle$), and red and white blood cell suspensions and blood plasma (*). The perturbation is with respect to a reference measurement of air.

where we have introduced A as a complex fitting parameter describing the sample volume and total stored energy and $B = 1$.

Ten binary solutions of ethanol and water with molar fractions of ethanol $\chi_{eth} = 0$, 0.04, 0.08, 0.11, 0.18, 0.3, 0.5, 0.7, 0.9, and 1.0 were used as calibration samples. It has previously been observed that the permittivity of ethanol-water solutions in the THz band do not follow ideal mixing laws[13] and instead we utilize published results[14] for their permittivity at these molar concentrations. Figure 3(a) shows the measured change in resonant frequency, with respect to air, against ϵ' for the ethanol-water solution. Figure 3(b) shows the measured change in the reciprocal Q-factor from air against ϵ'' for the binary solution. Also plotted are the results of full-wave simulations of the PCR and the QS model. The QS model described by (3) was fitted to the measured

response using the Levenberg-Marquardt algorithm[15] with fitting complex parameter $A = 2.5 \times 10^{-4} - i5.3 \times 10^{-6}$. It can be seen that good agreement between the three results is achieved for low loss liquids ($\tan\delta = \epsilon''/\epsilon' < 1$); however, there is an increasing deviation in the imaginary component for liquids with high loss tangents.

The discrepancy between the full-wave simulations and the QS model arising for high sample loss tangents can be explained as a consequence of the skin depth $\delta = 1/Im\{\tilde{k}\}$ of the liquid becoming comparable to the capillary diameter. This corresponds to the transition from the depolarization regime to the skin depth regime, where the electrostatic solution is no longer valid due to field screening effects.[16] This effect could be reduced by using a smaller diameter capillary tube at the expense of lower sensitivity.

To improve the fit in the high loss case we attempt a semi-empirical fit, where we let terms ϵ_q and B in (3) be additional fitting parameters. The former is justified on the basis that the capillary tube wall is very thin and the response is also influenced by the combined effect of the surrounding air and silicon. The values of A, B, and ϵ_q in (3) were determined by fitting the measured response of the PCR to the ten ethanol-water solutions, giving $A = 8.4 \times 10^{-4} - i1.5 \times 10^{-4}$, $B = 1.4 + i0.57$, and $\epsilon_q = 3.3 - i3.8$. Figure 3 shows the improved fit achieved using this semi-empirical model, particularly for the liquids with higher loss.

The fitted QS and semi-empirical models can now be used to describe the response of the PCR for a range of common permittivities of liquids. Figures 4(a) and 4(b) show color maps calculated using the semi-empirical model that relate the liquid's real and imaginary parts of relative permittivity to the change in resonant frequency and Q-factor, respectively, of the resonator with air as reference. It can be seen that the resonant frequency is strongly influenced by both the real and imaginary part of the sample permittivity, and the Q-factor is mostly affected by the imaginary component. Furthermore, the PCR has the highest sensitivity to low permittivity liquids with low loss.
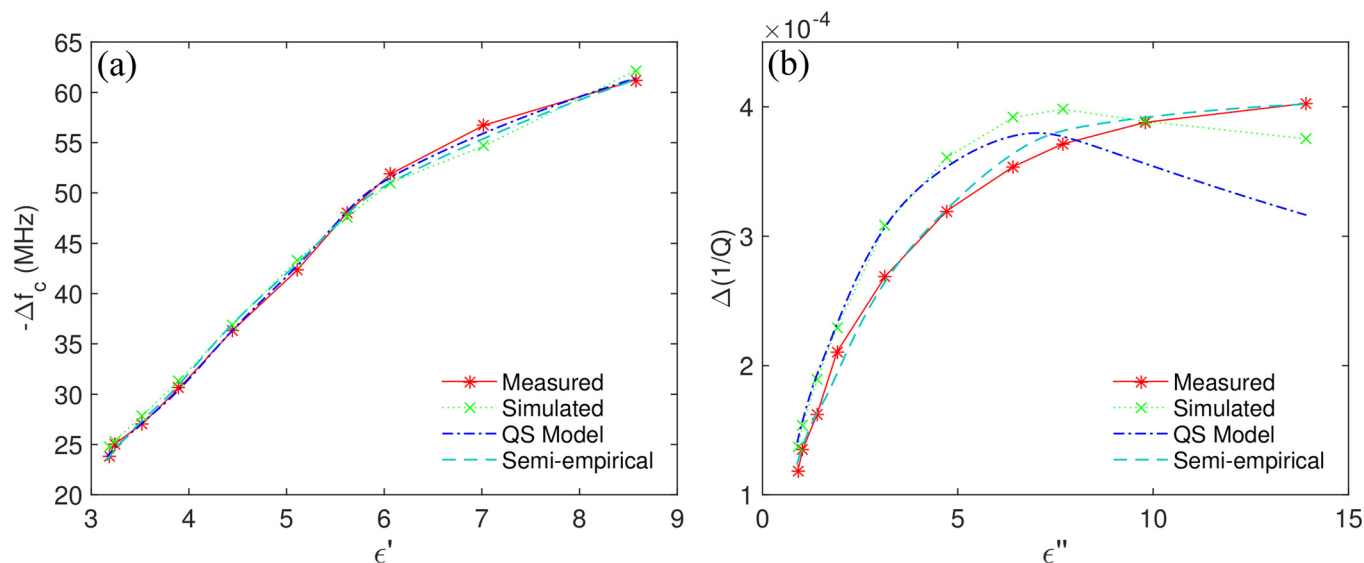

FIG. 3. (a) The change in resonance frequency of the PCR, with respect to air, against the real part of the relative permittivity of ethanol-water solutions of varying proportion. (b) The change in reciprocal Q-factor, with respect to air, against the imaginary part of the relative permittivity of the same ethanol-water solutions.
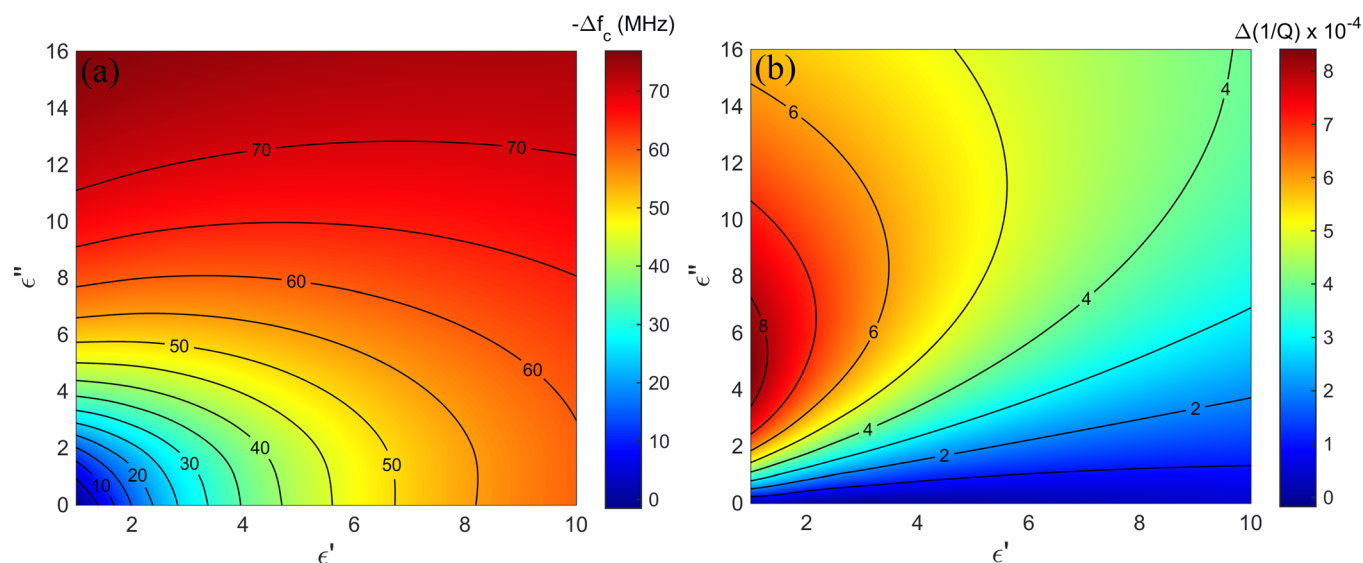
FIG. 4. Color maps showing the semi-empirical calculated perturbation in (a) resonant frequency and (b) reciprocal Q-factor as a function of the complex permittivity of the liquid sample.

Once the PCR response has been characterized using the ethanol-water solutions, the models can be used to estimate the complex permittivity for other liquids. Table I shows the permittivity for common solvents: methanol and 2-propanol estimated using the semi-empirical model. It can be seen that the method produces reasonably accurate values close to other reported values in the literature.[14,17,18]

A potentially significant source of error in these measurements is the thermal drift of the resonance, due to the temperature dependent permittivity of the silicon constituent of the PCR,[19] however, this effect can be minimized by making the reference and sample measurements as close together as possible. All measurements were undertaken at an ambient temperature of 296 K. Additionally, the semi-empirical model has an inherent inaccuracy compared to the calibration measurements that is worst for the case of high permittivity liquids, giving maximum errors of 4% and 14% in the real and imaginary parts of the relative permittivity, respectively, over the measured permittivity range.

Bioliquids are, in general, poorly characterized at terahertz frequencies and we next use the PCR to measure several bioliquids extracted from human blood. White and red blood cells were isolated using an Acrodisc WBC Syringe Filter (Pall Laboratory) by draining the blood through three 4.5 ml citrate coated vacutainers of whole blood and washing

with phosphate buffer solution (PBS). Isolated RBCs were then separated from plasma by centrifugation, followed by three PBS + 3% bovine serum albumin (BSA) washing and resuspension steps. WBCs were backwashed off the filter, run through another Acrodisc to remove remaining RBCs, and then the suspension centrifuged, washed, and resuspended three times with PBS + 3% BSA. The cell solutions were placed on an orbital shaker to help prevent cell aggregation. Cell sample concentrations were determined using a C-Chip (DigitalBio) haemocytometer and were estimated to be 0.4% for the WBC and 50% for the RBC by volume.

Table I shows the measured complex relative permittivities for the bioliquids. The plasma solution has a complex permittivity close to water, which is its primary constituent. The high frequency of measurement means that ionic conduction does not contribute to loss in these liquids. Solvated proteins have been shown to exhibit broad absorption spectra in the terahertz band, due to a high density of states of normal modes, however, this absorption is significantly less than bulk water.[20] The presence of proteins and other molecules in these liquids reduces the imaginary component of the permittivity, due to the higher loss of the displaced water. This difference can be seen in the smaller imaginary component of plasma (∼7% protein) when compared to water. Similarly, the RBC and WBC suspensions both have real parts of their permittivity close to water, with the RBC suspension having a significantly smaller imaginary component due to its protein content. In the case of the WBC suspension, the much lower concentration leads to only a minor difference in the imaginary component.

The volume of liquid interacting with the electric field of the resonant mode is estimated to be 3.6 nl, based on simulations. For a WBC mean corpuscular volume of 0.4 pl (Ref. 22) and concentration of 0.4% used in the WBC measurement, this corresponds to the probing of a suspension containing ∼40 cells. Future work aims at scaling the sensor to achieve a higher resonance frequency of >300 GHz, which would allow the terahertz dielectric response of individual cells to be probed with a proportionately smaller

TABLE I. Measured and literature values of the relative permittivities of liquids at 100 GHz.

Substance	Measured		Literature	
	ϵ'	ϵ''	ϵ'	ϵ''
Water[14]	8.5 ± 0.4	13.9 ± 2	8.6	13.9
Methanol[17]	4.0 ± 0.2	2.5 ± 0.4	4.6	2.0
Ethanol[14]	3.2 ± 0.2	0.9 ± 0.1	3.2	0.9
2-Propanol[18]	3.0 ± 0.2	0.6 ± 0.1	2.7	0.4
Plasma	8.7 ± 0.4	13.6 ± 2	…	…
RBC suspension[21]	8.2 ± 0.4	11.4 ± 2	8.3	11.4
WBC suspension	8.6 ± 0.4	14.2 ± 2	…	…

resonant mode volume. Improvements in sensitivity and device integration could also be obtained by integration of the microfluidic channel into the silicon substrate. Simulations show that by locating the liquid sample in a hole in the silicon in the middle of the PCR cavity, the sensitivity can be greatly improved, particularly for bio-liquids with permittivities close to water. The PCR could also be combined with a microfluidic droplet generator chip for the measurement of extremely small sample volumes by creating droplets of the sample immersed in a carrier fluid.

In conclusion, we have demonstrated a technique which exploits the high Q-factor of a PCR to provide highly sensitive measurements of nanoliter volumes of liquids in the terahertz band. The disposable nature of the capillary tubes makes this an attractive approach for the analysis of biological, toxic, or explosive liquids. This technique readily lends itself towards measurements at higher frequencies throughout the terahertz band and monolithic integration for lab-on-a-chip devices. Finally, we have provided estimates of the complex relative permittivity of several bioliquids that are constituents of human blood at 100 GHz.

[1]E. Chow, A. Grot, L. Mirkarimi, M. Sigalas, and G. Girolami, Opt. Lett. **29**, 1093 (2004).

[2]M. R. Lee and P. M. Fauchet, Opt. Express **15**, 4530 (2007).

[3]H. Ren, F. Vollmer, S. Arnold, and A. Libchaber, Opt. Express **15**, 17410 (2007).

[4]F. Vollmer and S. Arnold, Nat. Methods **5**, 591 (2008).

[5]E. N. Shaforost, N. Klein, S. A. Vitusevich, A. Offenhäusser, and A. A. Barannik, J. Appl. Phys. **104**, 074111 (2008).

[6]E. N. Shaforost, N. Klein, S. A. Vitusevich, A. A. Barannik, and N. T. Cherpak, Appl. Phys. Lett. **94**, 112901 (2009).

[7]W. J. Otter, S. M. Hanham, N. M. Ridler, G. Marino, S. Lucyszyn, and N. Klein, Sens. Actuators, A **217**, 151 (2014).

[8]Y. Akahane, T. Asano, B. Song, and S. Noda, Nature **425**, 944 (2003).

[9]A. F. Koenderink, M. Kafesaki, B. C. Buchler, and V. Sandoghdar, Phys. Rev. Lett. **95**, 153904 (2005).

[10]A. P. Gregory, "Q-factor Measurement Using a Vector Network Analyser," NPL Report No. MAT 58, 2013.

[11]L. F. Chen, C. K. Ong, C. P. Neo, V. V. Varadan, and V. K. Varadan, *Microwave Electronics: Measurement and Materials Characterization* (John Wiley and Sons, 2004), Chap. 6.

[12]See http://www.cst.com for more information regarding the frequency domain solver in CST Microwave Studio.

[13]P. Jepsen, U. Møller, and H. Merbold, Opt. Express **15**, 14717 (2007).

[14]T. Sato and R. Buchner, J. Phys. Chem. A **108**, 5007 (2004).

[15]K. Levenberg, Q. Appl. Math. **2**, 164–168 (1944).

[16]R. Inoue, H. Kitano, and A. Maeda, J. Appl. Phys. **93**, 2736 (2003).

[17]J. T. Kindt and C. A. Schmuttenmaer, J. Phys. Chem. **100**, 10373 (1996).

[18]J. Barthel, K. Bachhuber, R. Buchner, and H. Hetzenauer, Chem. Phys. Lett. **165**, 369 (1990).

[19]J. Krupka, J. Breeze, A. Centeno, N. Alford, T. Claussen, and L. Jensen, IEEE Trans. Microwave Theory Tech. **54**, 3995 (2006).

[20]J. Xu, K. W. Plaxco, and S. J. Allen, Protein Sci. **15**, 1175 (2006).

[21]Permittivity of whole blood given in: S. Gabriel, R. W. Lau, and C. Gabriel, Phys. Med. Biol. **41**, 2271 (1996).

[22]J. Gauthier, P. Harel, and C. Brosseau, Can. Med. Assoc. J. **109**, 3 (1973).